Supplemental Materials for Kuo, Zuo, et al.

The tight junction protein ZO-1 is dispensable for barrier function but critical for effective mucosal repair

Supplemental Table I.

GEO accession	GSE117993			GSE109142			GSE59071					GSE128682				
Sample size	55	43		20	206		11	74	23	control vs. active	active vs. inactive	16	14	14	control vs. active	active vs. inactive
Group	control	UC	*P*	control	UC	*P*	control	UC	inactive	*P*	*P*	control	UC	inactive	*P*	*P*
TJP2	27.16	23.42	$8.1x10^{-02}$	36.10	30.87	$2.9x10^{-02}$	9.22	9.05	9.19	$1.0x10^{-01}$	$1.9x10^{-02}$	11.73	11.47	12.14	$1.4x10^{-02}$	$6.1x10^{-06}$
OCLN	22.59	17.73	$8.5x10^{-03}$	34.26	17.65	$2.1x10^{-21}$	10.89	9.75	9.16	$1.2x10^{-04}$	$1.5x10^{-01}$	10.95	10.27	12.00	$1.6x10^{-05}$	$1.5x10^{-03}$
CLDN1	0.52	2.80	$1.6x10^{-08}$	0.47	3.39	$4.2x10^{-06}$	6.21	8.44	10.45	$5.2x10^{-13}$	$6.0x10^{-04}$	5.25	7.41	10.87	$2.7x10^{-07}$	$4.5x10^{-04}$
CLDN2	0.29	6.36	$1.1x10^{-11}$	0.16	5.76	$9.4x10^{-07}$	6.04	6.77	6.60	$1.3x10^{-09}$	$2.3x10^{-14}$	1.37	6.92	6.01	$3.1x10^{-15}$	$5.2x10^{-04}$
CLDN3	309.30	207.04	$1.5x10^{-06}$	322.72	180.30	$2.0x10^{-19}$	11.37	11.01	6.14	$9.1x10^{-02}$	$1.7x10^{-12}$	11.55	11.23	5.14	$6.6x10^{-02}$	$5.3x10^{-03}$
CLDN4	409.00	287.88	$4.0x10^{-08}$	447.60	244.71	$7.7x10^{-19}$	9.44	8.99	11.57	$2.6x10^{-02}$	$2.3x10^{-4}$	13.15	12.72	11.91	$1.2x10^{-02}$	$7.5x10^{-04}$
CLDN5	10.45	10.61	$8.5x10^{-01}$	7.39	9.40	$2.4x10^{-02}$	7.40	7.59	9.49	$4.4x10^{-03}$	$5.6x10^{-4}$	6.82	6.78	13.33	$8.1x10^{-01}$	$1.3x10^{-03}$
CLDN7	462.80	346.14	$2.2x10^{-07}$	450.29	305.30	$8.3x10^{-09}$	11.71	11.18	7.57	$5.3x10^{-02}$	$7.1x10^{-1}$	12.83	12.51	6.59	$8.1x10^{-02}$	$3.7x10^{-01}$
CLDN8	54.88	11.14	$2.8x10^{-13}$	108.01	8.24	$1.2x10^{-66}$	8.80	4.95	11.54	$9.7x10^{-17}$	$5.5x10^{-2}$	11.41	7.16	13.12	$1.0x10^{-05}$	$4.3x10^{-03}$
CLDN12	20.68	30.62	$1.5x10^{-05}$	25.98	37.58	$1.6x10^{-04}$	9.49	10.31	9.12	$9.5x10^{-06}$	$1.1x10^{-25}$	10.77	11.35	9.35	$3.1x10^{-05}$	$2.9x10^{-02}$
CLDN15	14.90	7.66	$6.4x10^{-13}$	8.78	6.62	$3.5x10^{-05}$	8.32	8.29	9.92	$3.0x10^{-01}$	$3.2 x10^{-3}$	7.98	7.20	11.14	$9.5x10^{-07}$	$2.1x10^{-01}$
CDH1	126.14	99.35	$7.0x10^{-04}$	159.09	94.27	$1.4x10^{-13}$	11.43	10.93	8.41	$5.3x10^{-02}$	$3.1x10^{-4}$	14.16	13.40	7.86	$3.0x10^{-06}$	$1.2x10^{-04}$

GEO accession	GSE87466			GSE117993			GSE59071			GSE93624			GSE101794		
Sample size	21	87		55	60		11	8		35	210		50	254	
Group	control	UC	*P*	control	CD	*P*	control	CD	*P*	control	CD	*P*	control	CD	*P*
TJP2	9.97	9.63	$2.2x10^{-04}$	27.16	26.23	$6.2x10^{-01}$	9.22	9.00	$2.4x10^{-02}$	4.52	4.35	$2.6x10^{-10}$	27.16	22.04	$4.2 x10^{-04}$
OCLN	8.21	7.51	$5.1x10^{-07}$	22.59	23.86	$4.7x10^{-01}$	10.89	10.02	$1.2x10^{-06}$	1.95	1.59	$2.1x10^{-16}$	18.68	12.40	$4.0 x10^{-08}$
CLDN1	4.85	6.34	$8.6x10^{-13}$	0.52	1.68	$7.2x10^{-05}$	6.21	7.70	$2.7x10^{-04}$	N.A.	N.A.	N.A.	0.57	1.57	$2.1 x10^{-05}$
CLDN2	5.32	7.58	$3.4x10^{-17}$	0.29	1.69	$1.9x10^{-03}$	6.04	6.35	$3.1x10^{-02}$	N.A.	N.A.	N.A.	14.92	23.51	$1.3 x10^{-05}$
CLDN3	8.46	8.02	$4.1x10^{-02}$	309.30	273.33	$5.5x10^{-02}$	11.37	11.20	$1.3x10^{-01}$	7.55	7.04	$2.0x10^{-12}$	113.92	92.70	$4.1 x10^{-03}$
CLDN4	9.755	9.45	$3.6x10^{-02}$	409.00	384.63	$2.6x10^{-01}$	9.44	9.08	$5.2x10^{-03}$	7.55	7.21	$1.0x10^{-06}$	108.42	102.23	$4.5 x10^{-01}$
CLDN5	7.56	7.81	$4.4x10^{-02}$	10.45	9.36	$1.7x10^{-01}$	7.40	7.59	$3.8x10^{-02}$	3.28	3.46	$4.1x10^{-03}$	9.70	10.45	$2.8 x10^{-01}$
CLDN7	10.89	10.32	$6.7x10^{-04}$	462.80	458.52	$8.4x10^{-01}$	11.71	11.44	$3.2x10^{-02}$	7.85	7.57	$6.0x10^{-07}$	292.96	270.04	$2.0 x10^{-01}$
CLDN8	9.53	5.85	$9.0x10^{-10}$	54.88	39.17	$6.5x10^{-03}$	8.80	6.06	$8.0x10^{-03}$	N.A.	N.A.	N.A.	1.53	1.23	$7.0 x10^{-01}$
CLDN12	9.43	9.89	$7.1x10^{-06}$	20.68	25.39	$9.7x10^{-03}$	9.49	10.01	$9.8x10^{-05}$	4.05	4.31	$9.2x10^{-09}$	13.92	17.62	$1.3 x10^{-03}$
CLDN15	7.27	6.43	$7.6x10^{-15}$	14.90	11.20	$2.5x10^{-05}$	8.32	8.21	$5.1x10^{-02}$	6.78	6.06	$2.2x10^{-20}$	171.55	102.75	$1.7 x10^{-11}$
CDH1	5.57	5.23	$6.7x10^{-05}$	126.14	121.74	$5.2x10^{-01}$	11.42	11.19	$1.6x10^{-02}$	6.74	6.40	$8.4x10^{-14}$	104.83	82.35	$1.4 x10^{-03}$

Supplemental Figures

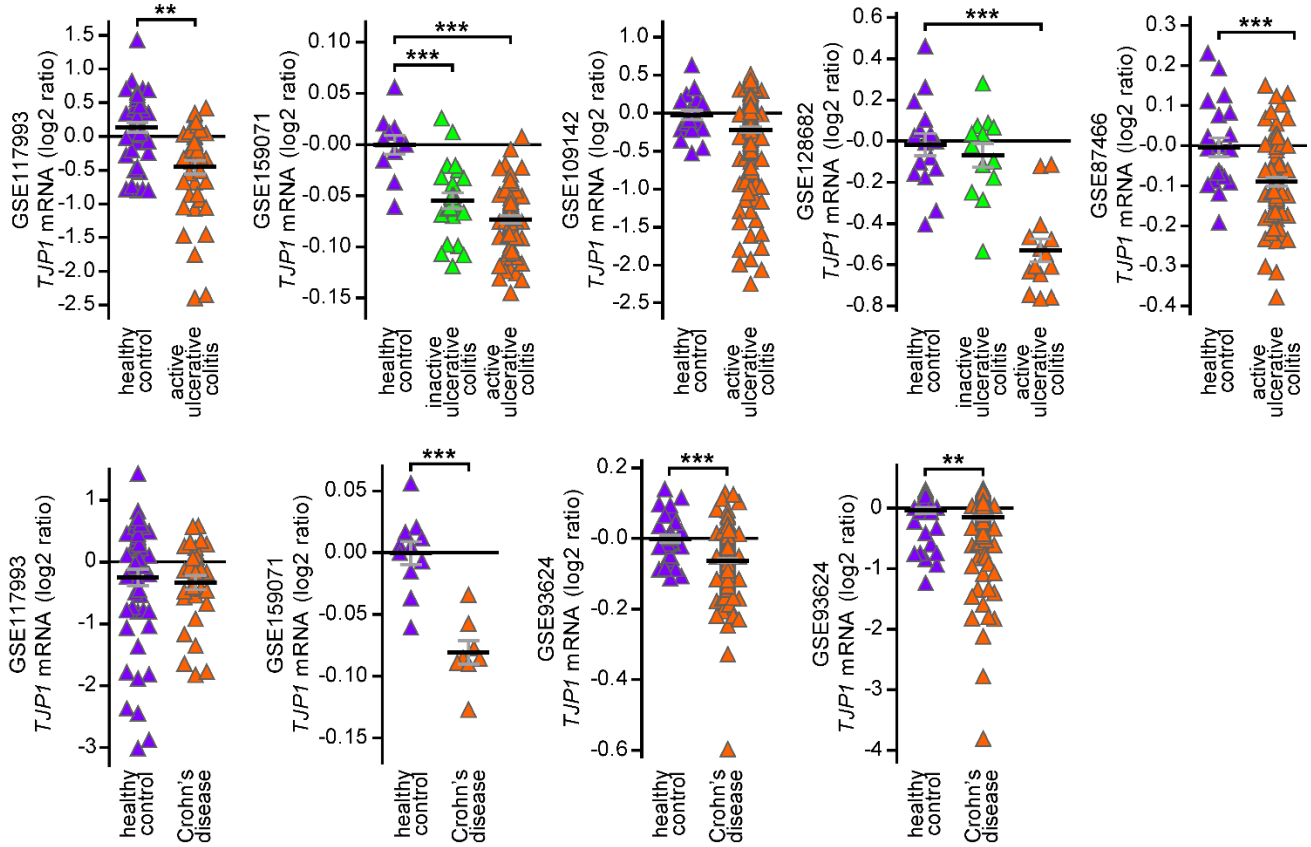

Supplemental figure 1. *TJP1* transcript expression in from five different GSE data sets, as indicated. Five of seven data sets show significantly reduced transcripts in patients (orange triangles) relative to healthy controls (purple triangles). Student's t test. ***, $P < .001$.

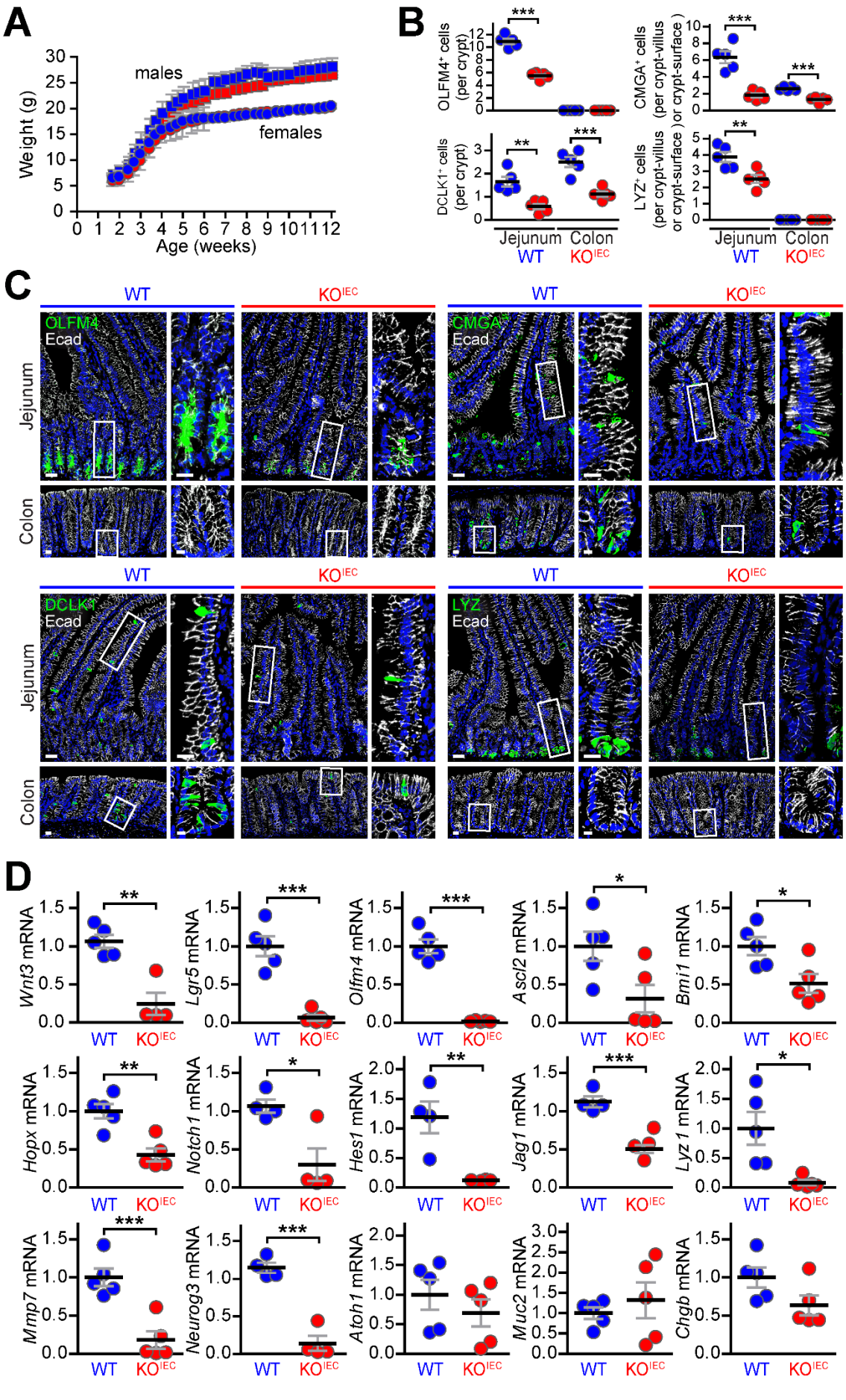
A
Weight (g)
Age (weeks)
males
females
B
OLFM4+ cells (per crypt)
CMGA+ cells (per crypt-villus or crypt-surface)
DCLK1+ cells (per crypt)
LYZ+ cells (per crypt-villus or crypt-surface)
Jejunum
Colon
WT
KOIEC
C
WT
KOIEC
OLFM4
Ecad
CMGA
DCLK1
LYZ
Jejunum
Colon
D
Wnt3 mRNA
Lgr5 mRNA
Olfm4 mRNA
Ascl2 mRNA
Bmi1 mRNA
Hopx mRNA
Notch1 mRNA
Hes1 mRNA
Jag1 mRNA
Lyz1 mRNA
Mmp7 mRNA
Neurog3 mRNA
Atoh1 mRNA
Muc2 mRNA
Chgb mRNA

Supplemental figure 2. ***A.*** Weight curves showing similar growth of male (squares) and female (circles) ZO-$1^{KO.IEC}$ (red) and WT (blue) mice. *n* =3 per group. ***B, C.*** Quantitative analysis of $OLFM4^+$, $DCLK1^+$, $CMGA^+$ (chromogranin), and LYZ^+ (lysozyme) cells in jejunum and colon of ZO-$1^{KO.IEC}$ (red circles) and WT (blue circles) mice. *n* = 5 per group. Photomicrographs of representative immunostains for each antigen (green) are shown. E-cadherin (white) and nuclei (blue) are shown for orientation ***D.*** qRT-PCR shows significantly reduced transcript expression of both stem and differentiated cell markers in jejunal epithelial cells from ZO-$1^{KO.IEC}$ relative to WT mice. *n* = 4-5 per group. Bars = 20 μm and 10 μm (high magnification). Student's t test. *, $P < .05$; **, $P < .01$; ***, $P < .001$.

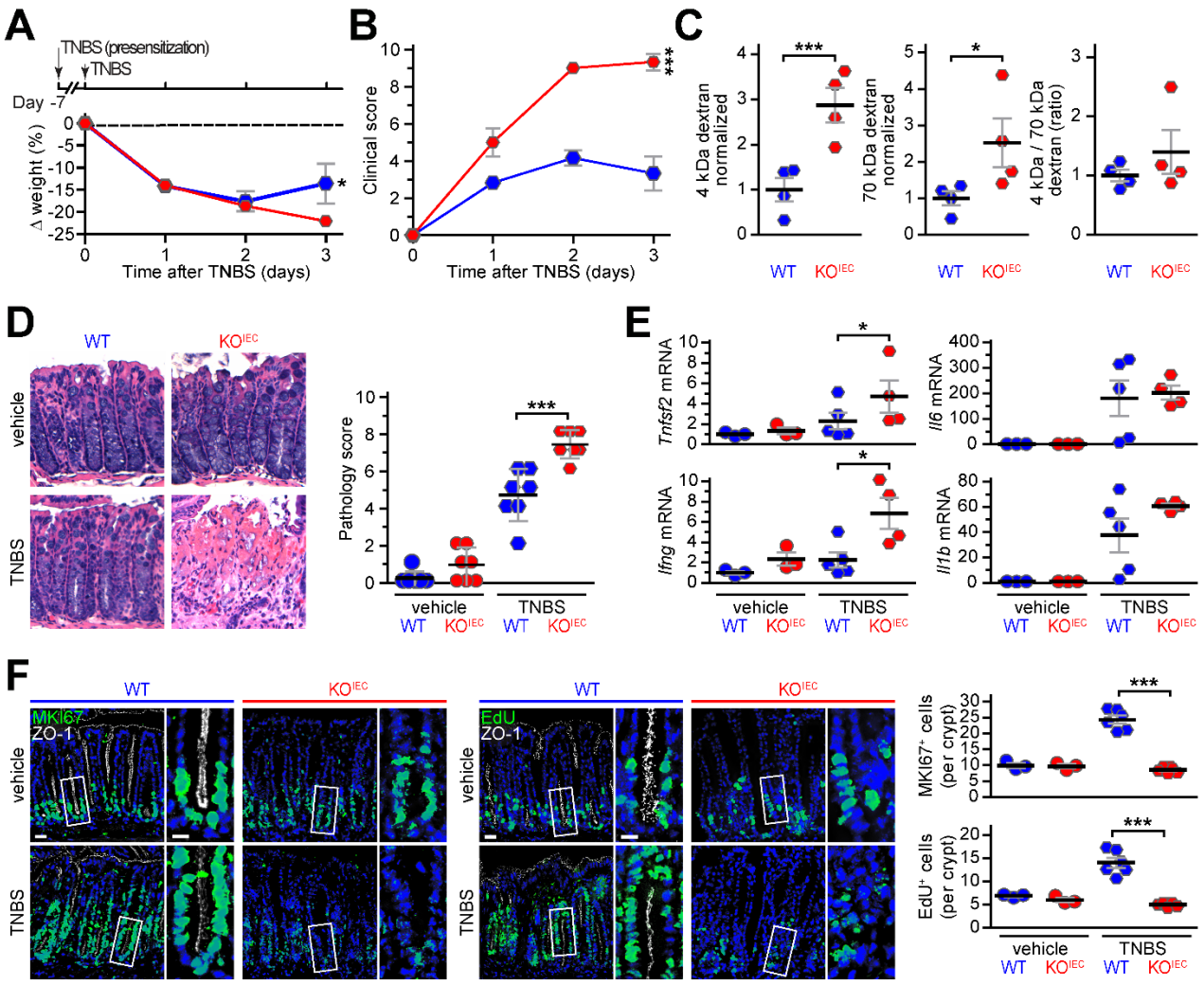

Supplemental figure 3. Mucosal repair is defective in TNBS-treated ZO-1$^{KO.IEC}$ mice. ***A, B.*** ZO-1$^{KO.IEC}$ (red) and WT (blue) mice were treated with TNBS and followed for 3 days. Weights and clinical scores are shown. *n* = 5 per group. ***C.*** Permeability of both 4 kDa dextran and 70 kDa dextran is dramatically increased in TNBS-treated ZO-1$^{KO.IEC}$, relative to WT, mice. The ratio of these probes is not changed, indicating that increased 4 kDa dextran permeability is due to mucosal damage. *n* = 4-5 per group. ***D.*** Representative images and histopathology scores of ZO-1$^{KO.IEC}$ and WT mice three days after TNBS treatment. *n* = 7 per group. ***E.*** qRT-PCR of mucosal transcripts before and after TNBS treatment shows significantly greater increases in *Tnsfr2* (TNF) and *Ifng* (IFNγ) in TNBS-treated ZO-1$^{KO.IEC}$, relative to WT, mice. *n* = 3-5 per group. ***F.*** MKI67 and EdU (green) stains show similar numbers of proliferating cells in ZO-1$^{KO.IEC}$ and WT

mice at baseline. However, TNBS only significantly increases proliferation in WT mice. ZO-1 (white) and nuclei (blue) are shown for orientation. *n* = 3-6 per group. Bars = 20 μm and 10 μm (high magnification). Student's t test (A-C) and ANOVA with Bonferroni's correction (D-F). *, $P < .05$; **, $P < .01$; ***, $P < .001$.

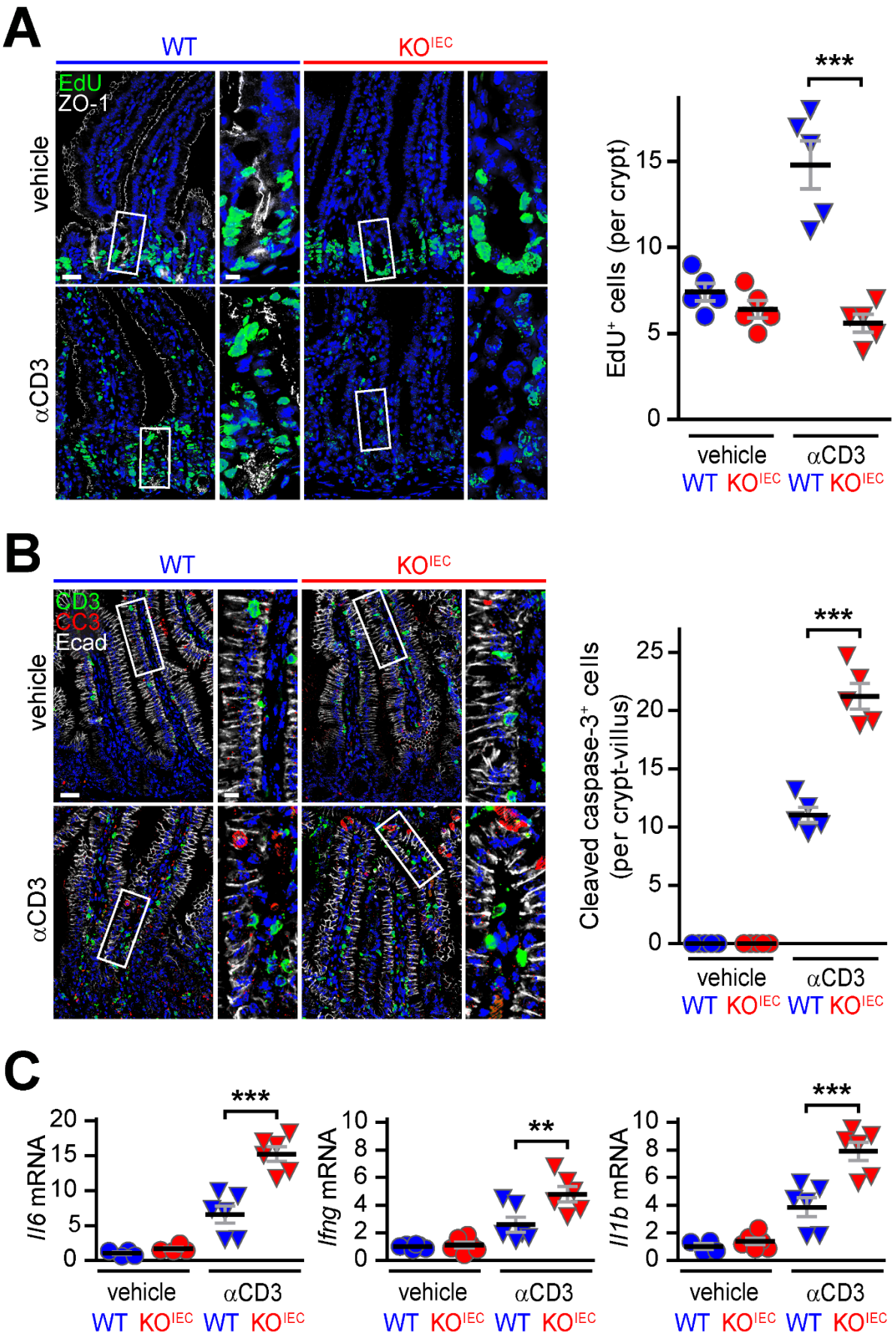
A
WT
KO^IEC
EdU
ZO-1
vehicle
αCD3
***
EdU⁺ cells (per crypt)
0
5
10
15
vehicle
αCD3
WT KO^IEC WT KO^IEC
B
WT
KO^IEC
CD3
CC3
Ecad
vehicle
αCD3
***
Cleaved caspase-3⁺ cells (per crypt-villus)
0
5
10
15
20
25
vehicle
αCD3
WT KO^IEC WT KO^IEC
C
Il6 mRNA
0
5
10
15
20
***
vehicle
αCD3
WT KO^IEC WT KO^IEC
Ifng mRNA
0
2
4
6
8
10
**
vehicle
αCD3
WT KO^IEC WT KO^IEC
Il1b mRNA
0
2
4
6
8
10
***
vehicle
αCD3
WT KO^IEC WT KO^IEC

Supplemental figure 4. Epithelial ZO-1 deletion diminishes proliferation, enhances apoptosis, and amplifies mucosal immune activation responses to T cell-induced mucosal injury. ***A.*** Numbers of EdU^+ cells (green) are similar in jejunal epithelial of ZO-$1^{KO.IEC}$ and WT mice at baseline. However, only WT mice are only able to significantly increase proliferation 2 days after anti-CD3 treatment. ZO-1 (white) and nuclei (blue) are shown for reference. *n* = 5 per group. ***B.*** ZO-1 deletion markedly increases T cell activation-induced epithelial apoptosis, detected as cleaved caspase-3 (red). E-cadherin (white), nuclei (blue), and CD3 (green) are shown for reference. *n* = 5 per group. ***C.*** qRT-PCR of mucosal transcripts before and 2 days after anti-CD3 treatment shows significantly greater increases in *Il6* (IL6), *Ifng* (IFNγ), and *Il1b* (IL1β) in anti-CD3-treated ZO-$1^{KO.IEC}$, relative to WT, mice. *n* =4-6 per group. Bars = 20 μm and 10 μm (high magnification). ANOVA with Bonferroni's correction. **, $P < .01$; ***, $P < .001$.

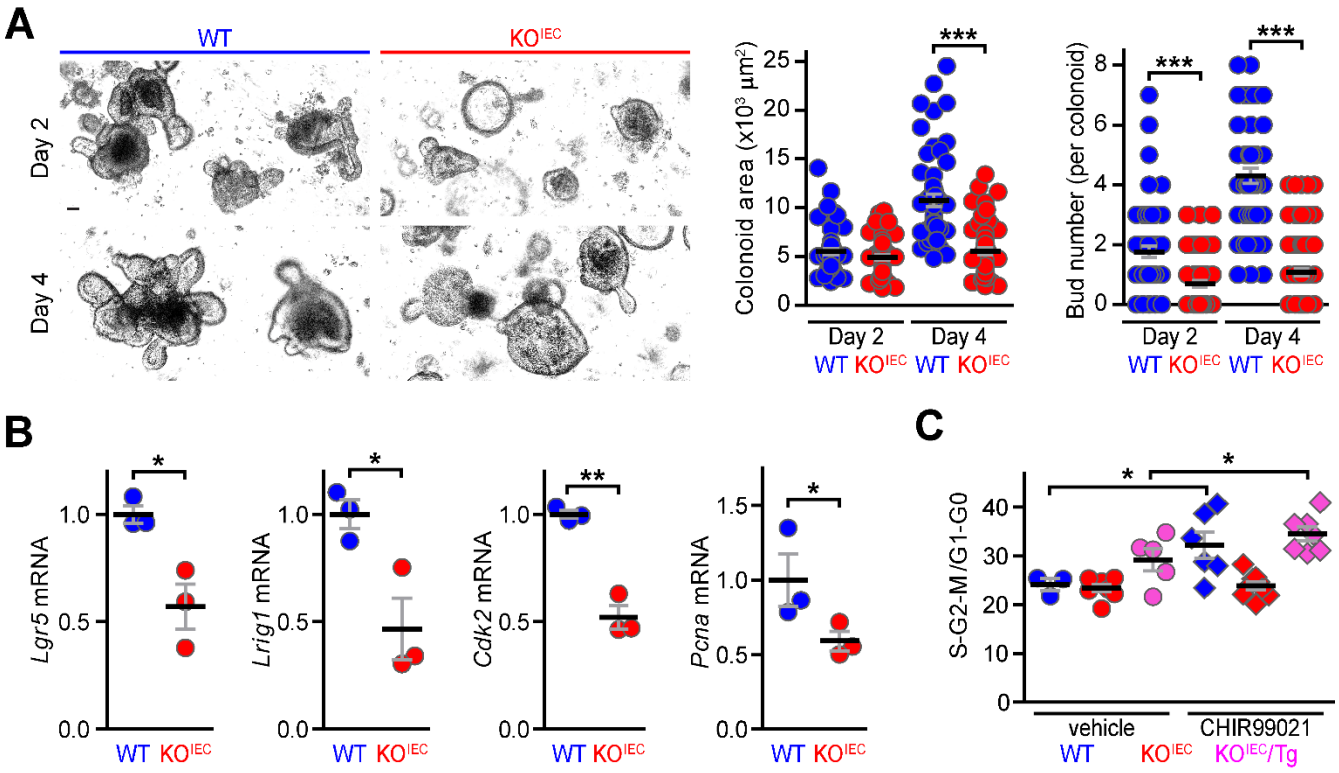

Supplemental figure 5. ZO-1 deletion reduces expression of stem cell and proliferative markers in colonoid cultures. *A.* Colonic epithelial stem cells were harvested from *Tjp1$^{f/f}$;* vil-Cre^{Tg} (ZO-1$^{KO.IEC}$) and *Tjp1$^{f/f}$* (WT) mice. Both cross-sectional area and bud number increased between days two and four in *Tjp1$^{f/f}$* but not *Tjp1$^{f/f}$;* vil-Cre^{Tg} colonoids. Bar = 20 µm. *n* = 52 per group. ***B.*** qRT-PCR shows reduced transcription of stem cell and proliferative markers in *Tjp1$^{f/f}$;* vil-Cre^{Tg} relative to *Tjp1$^{f/f}$* colonoids. *n* = 3 per group. ***C.*** Transgenic mRFP1-ZO-1 expression (vil-mRFP1-ZO-1^{Tg}; *Tjp1$^{f/f}$;* vil-Cre^{Tg} colonoids) rescues 5 µM CHIR99021-induced proliferation of *Tjp1$^{f/f}$;* vil-Cre^{Tg} colonoids. *n* = 3-9 per group. Student's t test (B). ANOVA with Bonferroni's correction (A, C). *, $P < .05$; **, $P < .01$; ***, $P < .001$.

Supplemental Materials and Methods

Mice and ARRIVE guidelines

All studies were performed according to protocols approved by the Institutional Animal Care and Use Committees of the Brigham and Women's Hospital and Boston Children's Hospital and made use of vil-mRFP1-ZO-1 (Tg(Vil1-mRFP1/TJP1)#Tjr, MGI:5584023)[1, 2], *Tjp1*$^{f/f}$ (*Tjp1*$^{tm2c(KOMP)Wtsi}$, MGI:6272009),[3] vil-Cre (B6.Cg-Tg(Vil1-cre)20Syr, MGI:3053819),[4] vil-CreERT2 (B6.Cg-Tg(Vil1-cre/ERT2)23Syr/J, MGI:6278020),[4] H2B-mCherry (R26-H2B-mCherry, CDB:CDB0239K),[5] and GFP-β-actin (*Pfn1*$^{tm2.1(GFP/ACTB)Wit}$, MGI:5568700)[6] mice. Crosses between these genotypes were used at 6 - 8 weeks of age to generate colonoids. Studies of live mice used 6 - 10 week old *Tjp1*$^{f/f}$-vil-Cre (ZO-1$^{KO.IEC}$) and *Tjp1*$^{f/f}$ (WT) littermates. Mice of both sexes were used, in separate experiments, for all studies. Numbers of mice in each study are provided in the figure legends. All experiments using mice were performed at least 3 times with similar results. Each figure presents data from a single independent experiment.

Human tissues

De-identified patient biopsies were obtained from the archives of the University of Chicago Hospitals and Brigham and Women's Hospital under IRB-approved protocols. Ileal biopsies from patients with established histories of Crohn's disease or left colonic biopsies from patients with established histories of ulcerative colitis were considered. Biopsies with extensive ulceration were excluded. Ileal and left colon biopsies without abnormalities from age- and sex-matched healthy patients, e.g., undergoing screening colonoscopies, were used as controls.

Human expression datasets

GDS3268, GSE117993, GSE59071, GSE128682, GSE87466, GSE59071, GSE93624, and GSE101794 mRNA chip and RNAseq datasets were downloaded from the NCBI Gene Expression Omnibus (GEO) repository.

Mucosal injury model

DSS (Alfa Aesar), 2% w/v unless specified, was added to drinking water for 6 days, as described.[7, 8] TNBS (Sigma-Millipore) colitis was induced 1 week after skin pre-sensitization, with 0.15 ml of 1% (w/v) TNBS solution in water/acetone/olive oil (16:4:5), by intrarectal administration of 0.1 ml of 2.5% TNBS (w/v) in 50% ethanol.[8, 9] Endotoxin-free Anti-CD3 (200 μg/mouse, clone 2C11, Bio X Cell) was injected intraperitoneally. Clinical scores were the sum of individual scores (0, 1, or 2) for activity, posture, fur texture, stool consistency, and fecal blood.

Imaging and post-acquisition analysis

Gross photos of colon were collected using a D90 camera with 40mm F2.8 AF-S lens (Nikon) and MF18 ring light (Nissin). Mucosae of 0.2% methylene blue-stained colons were imaged using a S8 APO dissecting microscope (Leica) equipped with a Micropublisher 3.3 camera (QImaging) controlled by QCapPro 6 software.

H&E-stained sections were imaged using a DMLB microscope (Leica) equipped with 20x NA 0.7 HC PLAN APO and 40x NA 0.65 HC FL PLAN objectives, a MicroPublisher 5.0 CCD camera (QImaging), and controlled by QCapPro 6. Histopathological scores of jejunal and colonic sections were the sum of individual scores (0, 1, 2) for goblet cell depletion, crypt cell apoptosis, epithelial erosion, lymphocytic infiltrate, and crypt architectural distortion.

Brightfield images of colonoids were acquired using a DM IL LED microscope (Leica) with 10x NA 0.25 N PLAN and 20x NA 0.4 HC PL FLUOTAR objectives and an AxioCam MRm CCD camera (Zeiss) controlled by AxioVision software (Zeiss). Colonoid area and bud numbers were quantified using AxioVision.

Fluorescent-stained tissue sections and epithelial cytopreps were imaged using either an Axioplan 2 microscope (Zeiss) with 20x NA 0.8 Plan-Apochromat and 63x NA 1.4 Plan-Apochromat objectives and a Coolsnap HQ (Photometrics) camera controlled by MetaMorph 7 (Molecular Devices) or a DM4000 microscope (Leica) with 20x NA 0.70 HC PLAN APO objective, 100X NA 1.35 HCX PL APO objective and Flash LT Plus (Hamamatsu) or CoolSnap HQ2 (Photometrics) camera controlled by Metamorph 7.

Both microscopes were equipped with ET filter cubes (49000, 49002, 49008, and 49009, Chroma Technology) and A SOLA UV LED light source (Lumencor).

Live colonoids, whole mounts of stained colonoids, and some tissue sections (Figure 7D) were imaged using a DM6000 microscope (Leica) with CSU-X1 spinning disk (Yokogawa), 20x NA 0.7 HC PLAN APO, 40x NA 0.75 HCX PL FLUOTAR, and 100x NA 1.4 HC PLAN APO CS2 objectives, and controlled by MetaMorph 7. For live imaging, the microscope was located within a 37°C heated enclosure and colonoids were grown in phenol red-free WENR media. In some experiments, nuclei were labeled with Nucspot 488 Live Nuclear Stain (Biotium) and an iXon Ultra 897 camera (Andor Technologies) was used to collect z-stacks with 2 µm steps at 10 min intervals. For imaging of fixed, stained colonoids, cytopreps, and some fluorescent-stained tissue sections, a Zyla 4.2 Plus sCMOS camera (Andor Technologies) was used to collect z-stacks with 0.5 µm steps.

Post-acquisition processing and analyses used MetaMorph 7, Autoquant X3 (MediaCybernetics), and Imaris 9.7 (Bitplane). For 3D reconstructions, colonoid z-stacks were processed using spot or surface tools. The spot tool was used with a radius of 2 to quantify numbers of Hoechst, EdU, or cleaved-caspase-3 stained cells. The surface tool with smoothing, grain size of 0.25 µm, and background subtraction was used to visualize the mRFP1-ZO-1 during cell division. Thresholding was performed manually.

Colonoid culture

Colonic crypts were isolated and cultured in growth factor reduced matrigel (Corning) with WENR medium contained basal media (Advanced Dulbecco modified Eagle medium/F12, 2 mM GlutaMAX, 100 mM HEPES, 100 µg/ml primocin, 1.25 mM N-acetyl cysteine, 1:100 B27 supplement, 1:200 N2 supplement, 50 ng/mL EGF) and 50% L-WRN conditioned medium.[10] ENR medium contained basal media with 15% R-spondin1 conditioned medium[11] and 100 ng/ml noggin. Medium was replaced every 2-3 days and organoids were passaged weekly. Where indicated, colonoids were treated with 1 µM 4-OH-tamoxifen (Thermo). CHIR99021 (Cayman) was used at 5 µM.

RNA isolation and quantitative RT-PCR

RNA was purified from epithelial cells, isolated as previously described[12, 13], or intestinal sections lysed in RLT buffer using RNeasy minicolumns (Qiagen). RNA quality was evaluated using the RNA 6000 Nano Kit and 2100 Bioanalyzer (Agilent Technologies). After digestion with RNase-free DNase, 1 μg of RNA was reverse transcribed and analyzed by qRT-PCR using SsoFast Universal SYBR (Bio-Rad) and a CFX96 thermocycler (Bio-Rad).

Primers used were:

Gene	Forward primer (5'-3')	Reverse primer (5'-3')
Tjp1	TGGAATTGCAATCTCTGGTG	CTGGCCCTCCTTTTAACACA
Tjp2	ATGGGAGCAGTACACCGTGA	TGACCACCCTGTCATTTTCTTG
Ocln	GCTGTGATGTGTGTGAGCTG	GACGGTCTACCTGGAGGAAC
Cldn2	GGCTGTTAGGCACATCCAT	TGGCACCAACATAGGAACTC
Cldn3	AAGCCGAATGGACAAAGAA	CTGGCAAGTAGCTGCAGTG
Cldn4	CGCTACTCTTGCCATTACG	ACTCAGCACACCATGACTTG
Cldn7	AGGGTCTGCTCTGGTCCTT	GTACGCAGCTTTGCTTTCA
Cldn8	GCCGGAATCATCTTCTTCAT	CATCCACCAGTGGGTTGTAG;
Tnfsf2	AGCCCCCAGTCTGTATCCTT	GGTCACTGTCCCAGCATCTT
Il1b	GAGTGTGGATCCCAAGCAAT	TACCAGTTGGGGAACTCTGC
Il6	CCGGAGAGGAGACTTCACAG	TCCACGATTTCCCAGAGAAC
Il17	TTCAGGGTCGAGAAGATGCT	AAACGTGGGGGTTTCTTAGG
Kc	TGTTGTGCGAAAAGAAGTGC	TACAAACACAGCCTCCCACA
Ifng	TCAAGTGGCATAGATGTGGAAGAA	TGGCTCTGCAGGATTTTCATG
Wnt3	TGGAACTGTACCACCATAGATGAC	ACACCAGCCGAGGCGATG
Lgr5	CCTACTCGAAGACTTACCCAGT	GCATTGGGGTGAATGATAGCA
Lrig1	TTGAGGACTTGACGAATCTGC	CTTGTTGTGCTGCAAAAAGAGAG
Olfm4	GCCACTTTCCAATTTCAC	GAGCCTCTTCTCATACAC
Ascl2	CTACTCGTCGGAGGAAAG	ACTAGACAGCATGGGTAAG

Bmi1	ATCCCCACTTAATGTGTGTCCT	CTTGCTGGTCTCCAAGTAACG
Hopx	ACCACGCTGTGCCTCATCGC	TTCTGACCGCCGCCACTCTG
Notch1	GATGGCCTCAATGGGTACAAG	TCGTTGTTGTTGATGTCACAGT
Hes1	TCAACACGACACCGGACAAAC	ATGCCGGGAGCTATCTTTCTT
Jag1	CCTCGGGTCAGTTTGAGCTG	CCTTGAGGCACACTTTGAAGTA
Lyz1	GGAATGGATGGCTACCGTGG	CATGCCACCCATGCTCGAAT
Mmp7	CTGCCACTGTCCCAGGAAG	GGGAGAGTTTTCCAGTCATGG
Neurog3	CCAAGAGCGAGTTGGCACT	CGGGCCATAGAAGCTGTGG
Atoh1	GAGTGGGCTGAGGTAAAAGAGT	GGTCGGTGCTATCCAGGAG
Muc2	ATGCCCACCTCCTCAAAGAC	GTAGTTTCCGTTGGAACAGTGAA
Chgb	GCTCAGCTCCAGTGGATAACA	CAGGGGTGATCGTTGGAACAC
Cdk2	CCCCAGAACCTGCTTATCAA	GCAGCCCAGAAGAATTTCAG
Pcna	CCACATTGGAGATGCTGTTG	CCGCCTCCTCTTCTTTATCC
Tacc3	TCAGAGACCCATCAGAAGTCCT	TCCAGGCCGACTCCTTAAAC
Aurka	TGCAAACGGATAGGGAAGGC	ACCGAAGGGAACAGTGGTCTTA
Cdk1	AATTGTGTTTTGCCACTCCCG	ACAGCGTCACTACCTCGTGT
Ube2c	TACCCTTACAACGCACCCAC	TCGATGTTGGGTTCTCCTAGC
Cdc25b	AGCCCCTGACTTGATGTGTC	AATGAGGTTCTCCATGCCCG
Rad23b	GGGAAAGATGCCTTTCCGGT	GGTCACTGCTTTGGGTTTTGT
Espl1	CGGCAGCTTCGAGGGAATTA	CTCATGGCAAAAGTCGCGG
Nek2	GGACATCCTGGAGCAGAAGG	CAGCCAGACATAGGAGCCTG
Plk1	GGTTTTCAATCGCTCCCAGC	AGGGGGTTCTCCACACCTTT
Top2a	TGGTTTTACGGAGCCAGTTTT	TCACGTCAGAGGTTGAGCAC
Cdh1	TCCTTGTTCGGCTATGTGTC	GGCATGCACCTAAGAATCAG
Krt8	TCTCCGAGATGAACCGCAAC	TTAATGGCCATCTCCCCACG

RNAseq and Gene set enrichment analysis (GSEA) analysis

RNA was isolated from jejunal epithelial cells[14] from untreated mice or mice sacrificed 2 and 4 days after anti-CD3 treatment, with multiple mice, as biological replicates, for each condition. RNA quality was evaluated using the RNA 6000 Nano Kit. RNA-seq libraries were generated using the Kapa stranded mRNA Hyper Prep Kit (Roche) to enrich polyA$^+$ transcripts. Deep sequencing was performed on the NextSeq 500 sequencing system (Illumina) with single-end 75bp sequencing. RNA-seq data analysis was performed using VIPER.[15] Differential gene expression analysis was performed using DESeq2.[16] Two-group comparisons were performed using Gene Set Enrichment Analysis software (version 4.1.0) and the molecular signatures database (version 7.4.0) to identify differentially expressed gene sets.[17-19]

Immunostaining

Formalin-fixed, paraffin-embedded mouse tissues were assembled into tissue microarrays before staining. After deparaffinization, 5-µm sections were rehydrated, and antigen was unmasked by heating in a pressure cooker to 100°C in 0.01 M citrate (pH 6.0) with 0.05% tween-20 (Dako) for 15 min. After cooling, sections were incubated in bleaching buffer (2.4 ml 1N NaOH, 30 ml 30% H_2O_2, 67.6 ml PBS) under a bright LED (broad spectrum) light for 1 hr at room temperature. The buffer was then replaced with fresh bleaching buffer and the sections were incubated under the light for 1 hr more. After one 10 min wash in PBS, sections were incubated with blocking buffer (Dako) for 20 min. Primary antibodies prepared in antibody diluent (Dako) were added overnight at room temperature. After three 10 min incubations with wash buffer (Dako), secondary antibodies prepared in antibody diluent were added for 1 hr. After washing and rinsing once in water, sections were mounted using Prolong Diamond.

Colonoids grown in Matrigel were fixed in 2% freshly-prepared paraformaldehyde in PBS for 30 min. They were then permeabilized using PBS with 0.5% Triton X-100, washed 3 times with PBS containing 100 mM glycine, and blocked by incubation in PBS with 10% normal donkey serum for 1 hr. Samples were then incubated overnight at 4° C in primary antibodies prepared in blocking buffer. After 6 washes, 15 min each, in wash buffer (0.2% Triton X-100, 0.1% BSA, 0.05% Tween 20), secondary antibodies prepared in blocking buffer were added for 1 hr at room temperature. After 6 additional washes, colonoids were rinsed once in water before mounting.

For preparation of epithelial cytopreps, freshly-harvested small intestinal mucosa was rinsed with PBS and it gently scraped using a microscope slide. This was then spread across a second slide, which was immediately dipped in -20° C methanol. After incubation at -20° C for 30 min,

Antibodies

Primary and secondary antibodies were used as follows:

Primary antibodies

Protein	Species	Source	RRID	Concentration
CD3	Rabbit	Abcam ab16669	AB_443425	1 μg/ml (IF)
CD68	Rabbit	Abcam ab125212	AB_10975465	1 μg/ml (IF)
CLDN2	Rabbit	Atlas HPA051548	AB_2681530	1 μg/ml (IF)
CLDN3	Rabbit	Thermo 34-1700	AB_2533158	2 μg/ml (IF)
Cleaved caspase-3	Rabbit	Cell Signaling 9664	AB_2070042	1 μg/ml (IF)
CMGA	Rabbit	Novus NB120-15160	AB_789299	2 μg/ml (IF)
DCLK1	Rabbit	Abcam ab109029	AB_10864128	1 μg/ml (IF)
E-cadherin	Mouse	Abcam ab76055	AB_1310159	1 μg/ml (IF)
LYZ	Rabbit	Abcam ab108508	AB_10861277	1 μg/ml (IF)
MKI67	Rabbit	Abcam ab16667	AB_302459	1 μg/ml (IF)
NaKATPase	Mouse	Abcam ab7671	AB_306023	5 μg/ml (IF)
NHE3	Rabbit	Novus NBP1-82574	AB_11038394	1 μg/ml (IF)
NUMA	Rabbit	Abcam ab86129	AB_10863280	1 μg/ml (IF)
OCLN	Rat	Clone 6B8A3	AB_2819194	1 μg/ml (IF)
OLFM4	Rabbit	Cell Signaling 39141	AB_2650511	1 μg/ml (IF)
Pericentrin	Rabbit	Novus NBP1-87772	AB_11018354	1 μg/ml (IF)
SGLT1	Rabbit	Abcam ab14686	AB_301411	1 μg/ml (IF)
ZO-1 (human)	Rat	Clone 6B6E4	AB_2783858	1 μg/ml (IF)
ZO-1 (mouse)	Rat	Clone R40.76	AB_2783859	1 μg/ml (IF) 0.1 μg/ml (WB)

Secondary antibodies

Description	Species	Source	RRID	Concentration
AF488-anti-rabbit IgG $F(ab')_2$	Donkey	Jackson ImmunoResearch 711-545-152	AB_2313584	3 μg/ml (IF)

AF594-anti-mouse IgG F(ab′)$_2$	Donkey	Jackson ImmunoResearch 715-585-150	AB_2340854	3 μg/ml (IF)
AF647-anti-rat IgG F(ab′)$_2$	Donkey	Jackson ImmunoResearch 712-605-153	AB_2340694	3 μg/ml (IF)
IRDye 800CW-anti-rat IgG	Goat	LI-COR Biosciences 925-32219	AB_2721932	0.1 μg/ml (WB)

Transmission electron microscopy

For transmission EM, tissue was fixed with 2.5% glutaraldehyde and 4% PFA in 100 mM sodium cacodylate buffer (pH 7.4), dehydrated, and embedded in Spurr resin prior to sectioning. Images were acquired on an FEI F30 transmission electron microscope (Tecnai).

Intestinal permeability

Mice were denied access to food but allowed water for 4 h prior to gavage with 0.25 ml saline containing 80 mg fluorescein-4 kDa dextran (Sigma-Millipore) and 4 mg rhodamine B-70 kDa dextran (Sigma-Millipore). Serum was collected after 3 hr, as described.[20] Recovery of fluorescein and rhodamine B probes were measured using excitation wavelengths of 495 nm and 555 nm and emission wavelengths of 525 nm and 585 nm, respectively, using a Synergy H1 multimode plate reader (BioTek).

Proliferation and apoptosis assays

Mice were injected with 5 mg/kg EdU (Cayman) and sacrificed after 2hr, 24hr, or 48hr. Tissues were fixed in formalin, paraffin-embedded, and sectioned. Colonoids were incubated with 1 μM EdU for 2hr or 24hr before fixation with 2% freshly-prepared paraformaldehyde (PFA) in PBS for 30 min. Both were stained using the Click-iT EdU Imaging Kit (Invitrogen) and analyzed as above.

Colonoids were dissociated with TrypLE Express (Invitrogen) supplemented with 10 μM Y-27632 (Thermo) for 20 minutes at 37°C. Clumps were removed using a 35 μm cell strainer (Thermo) and pelleted at 300 x *g* at 4°C for 5 minutes. For cell cycle analysis, cells were fixed in -20°C 70% ethanol, labeled with propidium iodide (50 μg/ml, Thermo), treated with 0.5 μg/ml RNase A (Sigma-Millipore), and resuspended in PBS prior to analysis. To assess apoptosis, live cells were treated with PO-PRO-1 and 7-AAD (Thermo). Staining was detected using a FACS LSRFortessa (BD Biosciences) and analyzed using FlowJo 9 software.

Statistics

All data are presented as mean ± SD and are representative of at least 3 independent experiments. In addition, each in vitro experiment evaluated colonoids within at least 3 separate wells. Statistical significance was determined by 2-tailed Student's t test or ANOVA with Bonferroni's correction, as indicated in the figure legends. Results with *P* less than .05 were considered significant. In all figures, *, $P < .05$; **, $P < .01$; ***, $P < .001$.

Supplemental references

1. Marchiando AM, Shen L, Graham WV, et al. Caveolin-1-dependent occludin endocytosis is required for TNF-induced tight junction regulation in vivo. J Cell Biol 2010; 189:111-26.
2. Marchiando AM, Shen L, Graham WV, et al. The epithelial barrier is maintained by in vivo tight junction expansion during pathologic intestinal epithelial shedding. Gastroenterology 2011; 140:1208-1218 e1-2.
3. Odenwald MA, Choi W, Kuo WT, et al. The scaffolding protein ZO-1 coordinates actomyosin and epithelial apical specializations in vitro and in vivo. J Biol Chem 2018; 293:17317-17335.
4. el Marjou F, Janssen KP, Chang BH, et al. Tissue-specific and inducible Cre-mediated recombination in the gut epithelium. Genesis 2004; 39:186-93.
5. Abe T, Kiyonari H, Shioi G, et al. Establishment of conditional reporter mouse lines at ROSA26 locus for live cell imaging. Genesis 2011; 49:579-90.
6. Gurniak CB, Witke W. HuGE, a novel GFP-actin-expressing mouse line for studying cytoskeletal dynamics. Eur J Cell Biol 2007; 86:3-12.
7. Raju P, Shashikanth N, Tsai PY, et al. Inactivation of paracellular cation-selective claudin-2 channels attenuates immune-mediated experimental colitis in mice. J Clin Invest 2020; 130:5197-5208.
8. Kuo WT, Shen L, Zuo L, et al. Inflammation-induced Occludin Downregulation Limits Epithelial Apoptosis by Suppressing Caspase-3 Expression. Gastroenterology 2019; 157:1323-1337.
9. Waldner MJ, Neurath MF. Chemically induced mouse models of colitis. Curr Protoc Pharmacol 2009; Chapter 5:Unit 5 55.
10. Miyoshi H, Stappenbeck TS. In vitro expansion and genetic modification of gastrointestinal stem cells in spheroid culture. Nat Protoc 2013; 8:2471-82.
11. Ootani A, Li X, Sangiorgi E, et al. Sustained in vitro intestinal epithelial culture within a Wnt-dependent stem cell niche. Nat Med 2009; 15:701-6.
12. Nik AM, Carlsson P. Separation of intact intestinal epithelium from mesenchyme. Biotechniques 2013; 55:42-4.

13. Tsai PY, Zhang B, He WQ, et al. IL-22 Upregulates Epithelial Claudin-2 to Drive Diarrhea and Enteric Pathogen Clearance. Cell Host Microbe 2017; 21:671-681 e4.
14. Jadhav U, Cavazza A, Banerjee KK, et al. Extensive Recovery of Embryonic Enhancer and Gene Memory Stored in Hypomethylated Enhancer DNA. Mol Cell 2019; 74:542-554 e5.
15. Cornwell M, Vangala M, Taing L, et al. VIPER: Visualization Pipeline for RNA-seq, a Snakemake workflow for efficient and complete RNA-seq analysis. BMC Bioinformatics 2018; 19:135.
16. Love MI, Huber W, Anders S. Moderated estimation of fold change and dispersion for RNA-seq data with DESeq2. Genome Biol 2014; 15:550.
17. Subramanian A, Tamayo P, Mootha VK, et al. Gene set enrichment analysis: A knowledge-based approach for interpreting genome-wide expression profiles. Proceedings of the National Academy of Sciences 2005; 102:15545-15550.
18. Liberzon A, Birger C, Thorvaldsdottir H, et al. The Molecular Signatures Database (MSigDB) hallmark gene set collection. Cell Syst 2015; 1:417-425.
19. Liberzon A, Subramanian A, Pinchback R, et al. Molecular signatures database (MSigDB) 3.0. Bioinformatics 2011; 27:1739-40.
20. Chanez-Paredes SD, Abtahi S, Kuo W-T, et al. Differentiating Between Tight Junction-Dependent and Tight Junction-Independent Intestinal Barrier Loss In Vivo. Methods in Molecular Biology: Springer US, 2021.